Inorg. Chem. **2009**, *48*, 3065−3072

Exploring the Effects of Reduction or Lewis Acid Coordination on the U═O Bond of the Uranyl Moiety

Trevor W. Hayton* and Guang Wu

Department of Chemistry and Biochemistry, University of California Santa Barbara, Santa Barbara, California 93106

Received December 10, 2008

Reaction of Li(Ar*N*C(Ph)CHC(Ph)*O*) (^{Ar}acnac; Ar = 2,4,6-$Me_3C_6H_2$) or Na(Ar*N*C(Ph)CHC(Ph)*O*) (Ar = 3,5-^{t}Bu$_2$C$_6$H$_3$) with 0.5 equiv of $UO_2Cl_2(THF)_3$ results in the formation of $UO_2(^{Ar}acnac)_2$ (Ar = 2,4,6-$Me_3C_6H_2$, **1**; 3,5-^{t}Bu$_2$C$_6$H$_3$, **2**), which were isolated as orange crystalline solids in good yields. The structure of **2** has been confirmed by X-ray crystallography, while the solution redox properties of **1** and **2** have been measured by cyclic voltammetry. Complex **1** exhibits a reversible reduction feature at $E_{1/2} = -1.52$ V (vs Fc/Fc^+), while complex **2** exhibits a reduction feature at −1.35 V (vs Fc/Fc^+). Complexes **1** and **2** react with Cp^*_2Co to generate $[Cp^*_2Co][UO_2(^{Ar}acnac)_2]$ (Ar = 2,4,6-$Me_3C_6H_2$, **3**; 3,5-^{t}Bu$_2$C$_6$H$_3$, **4**), in moderate to good yields. Both **3** and **4** have been fully characterized, while the structure of **4** has also been determined by X-ray crystallography. Reaction of **2** with 2 equiv of $B(C_6F_5)_3$ in CH_2Cl_2 leads to the isolation of $UO(OB\{C_6F_5\}_3)(^{Ar}acnac)_2$ (Ar = 3,5-^{t}Bu$_2$C$_6$H$_3$) (**5**). Complex **5**, generated in situ, exhibits an irreversible reduction at −0.78 V (vs Fc/Fc^+, 100 mV/s scan rate) which is considerably lower than the reduction potential observed for **2**, consistent with the removal of electron density from the uranyl moiety by coordination of $B(C_6F_5)_3$.

Introduction

Uranyl (UO_2^{2+}) is an exceptionally stable molecular species, characterized by a linear O═U═O geometry, short U−O bonds (ca. 1.78 Å), and substitutionally inert oxo ligands.[1] Because of this extraordinary stability, selective functionalization of the uranyl oxo ligands is relatively rare. However, several recent examples demonstrate that functionalization is possible. For instance, coordination of two potassium cations to one of the oxo ligands in a uranyl macrocycle complex induces the reductive silylation of the uranyl moiety,[2] causing a notable lengthening of the functionalized U−O bond. Coordination of the strong Lewis acid $B(C_6F_5)_3$ to one of the oxo ligands of uranyl also causes a marked change to the uranyl fragment, increasing in the U−O bond length of the coordinated oxo by about 0.1 Å.[3] In contrast, the coordination of weaker Lewis acids to uranyl, such as alkali metal cations or 3d transition metals, does not induce much change in the U−O bond length.[4−6] The uranyl moiety can also be perturbed upon reduction to uranium(V). For example, structural studies of $[UO_2(py)_5][KI_2(py)_2]$,[7,8] $[UO_2(OPPh_3)_4][OTf]$,[9] and $\{[UO_2(dbm)_2]_4[K_6(py)_{10}]\}^{2+}$[10] all reveal slightly longer U−O(oxo) bonds than those observed for UO_2^{2+};[1,11] however, the O−U−O angles are still 180°. Processes that effect the complete substitution of the uranyl oxo ligands are equally uncommon and are usually limited to photochemical-mediated reactions,[12] microbial activity,[13−15] or powerful reducing agents.[16]

In this contribution we report the synthesis and characterization of two uranyl(V) bis(β-ketoiminate) complexes, namely, $[Cp^*_2Co][UO_2(^{Ar}acnac)_2]$ (Ar = 2,4,6-$Me_3C_6H_2$, 3,5-^{t}Bu$_2$C$_6$H$_3$). These complexes contain the rare $U^VO_2^+$ moiety, which has

* To whom correspondence should be addressed. E-mail: hayton@chem.ucsb.edu.

(1) Denning, R. G. *J. Phys. Chem. A* **2007**, *111*, 4125–4143.
(2) Arnold, P. L.; Patel, D.; Wilson, C.; Love, J. B. *Nature* **2008**, *451*, 315–317.
(3) Sarsfield, M. J.; Helliwell, M. *J. Am. Chem. Soc.* **2004**, *126*, 1036–1037.
(4) Burns, C. J.; Clark, D. L.; Donohoe, R. J.; Duval, P. B.; Scott, B. L.; Tait, C. D. *Inorg. Chem.* **2000**, *39*, 5464–5468.
(5) Arnold, P. L.; Patel, D.; Blake, A. J.; Wilson, C.; Love, J. B. *J. Am. Chem. Soc.* **2006**, *128*, 9610–9611.
(6) Berard, J. J.; Schreckenbach, G.; Arnold, P. L.; Patel, D.; Love, J. B. *Inorg. Chem.* **2008**, *47*, 11583–11592.
(7) Natrajan, L.; Burdet, F.; Pécaut, J.; Mazzanti, M. *J. Am. Chem. Soc.* **2006**, *128*, 7152–7153.
(8) Berthet, J.-C.; Siffredi, G.; Thuéry, P.; Ephritikhine, M. *Chem. Commun.* **2006**, 3184–3186.
(9) Berthet, J.-C.; Nierlich, M.; Ephritikhine, M. *Angew. Chem., Int. Ed.* **2003**, *42*, 1952–1954.

10.1021/ic802360y CCC: $40.75
Published on Web 03/05/2009

recently been the focus of increased study.[7,8,10,17−24] This fragment readily disproportionates to UO_2^{2+} and U^{4+},[25] a property that has previously hampered its isolation and characterization. We have also explored the reactivity of the uranyl(VI) precursors, $UO_2(^{Ar}acnac)_2$, with $B(C_6F_5)_3$. This has provided us with the unprecedented opportunity to evaluate the structural deformations of the uranyl moiety induced by either reduction or Lewis acid coordination to an "yl" oxygen, while keeping the equatorial ligand environment identical. These two modes of reactivity may also provide a pathway by which further functionalization of uranyl can be achieved. By studying these interactions and discovering methods to effect the functionalization of uranyl oxo ligands, we hope to develop novel strategies for waste treatment and environmental remediation.

Results and Discussion

We have previously used a β-diketiminate ligand to stabilize the UO_2^+ fragment.[18,19] However, these complexes are thermally unstable, possibly because of the relatively acidic methyl protons on the ligand backbone.[18,26−30] Thus, we have endeavored to find a new ligand platform with similar electronic and steric properties as the β-diketiminates but without the methyl substituents attached to the β carbons of the ligand skeleton. In this regard, the diphenyl-β-ketoiminate ligands are an attractive option. This framework can be synthesized by condensation of a substituted-aniline with dibenzoylmethane, under solventless conditions,[31] or in refluxing toluene.[32] In this fashion we can easily construct, in one step, a β-ketoimine with robust phenyl substituents attached at the β-positions. Several transition-metal β-ketoiminate complexes have been isolated,[33] and this ligand architecture has been successfully used to build Ti-based olefin polymerization catalysts[34] and Ni-based methyl methacrylate polymerization catalysts.[35] In addition, the related diphenyl-β-diketonate ligand set has been previously used to stabilize U(V). For example, the solid-state molecular structures of $\{[UO_2(dbm)_2]_2[\mu\text{-}K(py)_2]_2[\mu_8\text{-}K(py)]\}_2^{2+}$ and $\{[UO_2(dbm)_2][K(18\text{-crown-}6)]\}_2$ were recently determined.[10,22] Each complex is built from the $[U^VO_2(dbm)_2]^-$ fragment and held together with bridging uranyl-oxo interactions. Furthermore, in situ reduction of $UO_2(dbm)_2(DMSO)$ leads to the formation of $[UO_2(dbm)_2(DMSO)]^-$.[36,37] These examples provide further justification for using the ketoiminate ligand architecture.

Condensation of mesitylaniline or 3,5-di-*tert*-butylaniline with dibenzoylmethane in refluxing toluene, using $Zn(OTf)_2$ as a catalyst, results in the isolation of H(Ar*N*C(Ph)CHC(Ph)*O*) (H(^{Ar}acnac); Ar = 2,4,6-$Me_3C_6H_2$, 3,5-$^tBu_2C_6H_3$), in modest to good yields (eq 1). Alternately, the condensation of 3,5-di-*tert*-butylaniline with dibenzoylmethane can also be performed under solvent-less conditions. The condensation of bulkier arylamines, such as 2,6-diisopropylaniline, with dibenzoylmethane was not observed under these conditions, presumably because of the steric bulk of the isopropyl substitutents. In addition, we observe no evidence for the formation of a β-diketimine.

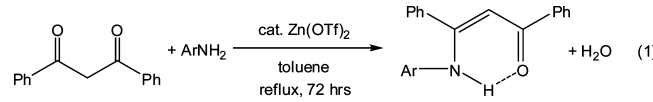

Ar = 2,4,6-$Me_3C_6H_2$, 3,5-$^tBu_2C_6H_3$

Deprotonation of the diphenyl-β-ketoimines is easily achieved by reaction with either *n*-BuLi or $NaN\{SiMe_3\}_2$. Subsequent addition of the alkali metal salt to 0.5 equiv of $UO_2Cl_2(THF)_3$ results in the formation of $UO_2(^{Ar}acnac)_2$ (Ar = 2,4,6-$Me_3C_6H_2$, **1**; 3,5-$^tBu_2C_6H_3$, **2**), which were isolable as orange crystalline solids in good yields (eq 2).

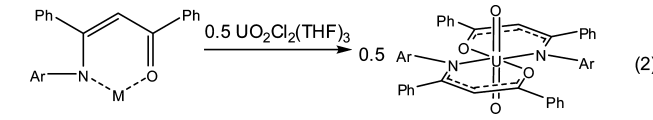

M = Li, Ar = 2,4,6-$Me_3C_6H_2$
M = Na, Ar = 3,5-$^tBu_2C_6H_3$

Ar = 2,4,6-$Me_3C_6H_2$, **1**; 3,5-$^tBu_2C_6H_3$, **2**

Complexes **1** and **2** are soluble in toluene, tetrahydrofuran (THF), and CH_2Cl_2. Complex **1** exhibits two singlets in a 2:1 ratio at 2.23 and 2.42 ppm, respectively, in its ^{1}H NMR spectrum in CD_2Cl_2, which corresponds to the mesityl methyl groups. **1** also exhibits a singlet at 6.15 ppm assignable to the proton attached to the γ-carbon of the ketoiminate ring. Similarly, complex **2** exhibits a singlet at 1.11 ppm in its ^{1}H NMR spectrum in CD_2Cl_2, which corresponds to the methyl

(10) Burdet, F.; Pecaut, J.; Mazzanti, M. *J. Am. Chem. Soc.* **2006**, *128*, 16512–16513.
(11) Denning, R. G. *Struct. Bonding (Berlin)* **1992**, *79*, 215–276.
(12) Kannan, S.; Vaughn, A. E.; Weis, E. M.; Barnes, C. L.; Duval, P. B. *J. Am. Chem. Soc.* **2006**, *128*, 14024–14025.
(13) Sundararajan, M.; Campbell, A. J.; Hillier, I. H. *J. Phys. Chem. A* **2008**, *112*, 4451–4457.
(14) Renshaw, J. C.; Butchins, L. J. C.; Livens, F. R.; May, I.; Charnock, J. M.; Lloyd, J. R. *Environ. Sci. Technol.* **2005**, *39*, 5657–5660.
(15) Lovley, D. R.; Phillips, E. J. P.; Gorby, Y. A.; Landa, E. R. *Nature* **1991**, *350*, 413–416.
(16) Berthet, J. C.; Siffredi, G.; Thuery, P.; Ephritikhine, M. *Eur. J. Inorg. Chem.* **2007**, 4017–4020.
(17) Yamamura, T.; Shirasaki, K.; Sato, H.; Nakamura, Y.; Tomiyasu, H.; Satoh, I.; Shiokawa, Y. *J. Phys. Chem. C* **2007**, *111*, 18812–18820.
(18) Hayton, T. W.; Wu, G. *Inorg. Chem.* **2008**, *47*, 7415–7423.
(19) Hayton, T. W.; Wu, G. *J. Am. Chem. Soc.* **2008**, *130*, 2005–2014.
(20) Steele, H.; Taylor, R. J. *Inorg. Chem.* **2007**, *46*, 6311–6318.
(21) Ikeda, A.; Hennig, C.; Tsushima, S.; Takao, K.; Ikeda, Y.; Scheinost, A. C.; Bernhard, G. *Inorg. Chem.* **2007**, *46*, 4212–4219.
(22) Nocton, G.; Horeglad, P.; Pecaut, J.; Mazzanti, M. *J. Am. Chem. Soc.* **2008**, *130*, 16633–16645.
(23) Mizuoka, K.; Grenthe, I.; Ikeda, Y. *Inorg. Chem.* **2005**, *44*, 4472–4474.
(24) Mizuoka, K.; Ikeda, Y. *Inorg. Chem.* **2003**, *42*, 3396–3398.
(25) Ekstrom, A. *Inorg. Chem.* **1974**, *13*, 2237–2241.
(26) Hitchcock, P. B.; Lappert, M. F.; Protchenko, A. V. *Chem. Commun.* **2005**, 951–953.
(27) Basuli, F.; Huffman, J. C.; Mindiola, D. J. *Inorg. Chem.* **2003**, *42*, 8003–8010.
(28) Neculai, A. M.; Roesky, H. W.; Neculai, D.; Magull, J. *Organometallics* **2001**, *20*, 5501–5503.
(29) Ding, Y.; Hao, H.; Roesky, H. W.; Noltemeyer, M.; Schmidt, H. G. *Organometallics* **2001**, *20*, 4806–4811.
(30) Mindiola, D. J. *Acc. Chem. Res.* **2006**, *39*, 813–821.
(31) Zhang, Z.-H.; Yin, L.; Wang, Y.-M. *Adv. Synth. Catal.* **2006**, *348*, 184–190.
(32) Bartoli, G.; Bosco, M.; Locatelli, M.; Marcantoni, E.; Melchiorre, P.; Sambri, L. *Synlett* **2004**, 239–242.
(33) Hsu, S. H.; Chang, J. C.; Lai, C. L.; Hu, C. H.; Lee, H. M.; Lee, G. H.; Peng, S. M.; Huang, J. H. *Inorg. Chem.* **2004**, *43*, 6786–6792.
(34) Li, X. F.; Dai, K.; Ye, W. P.; Pan, L.; Li, Y. S. *Organometallics* **2004**, *23*, 1223–1230.
(35) Li, X. F.; Li, Y. G.; Li, Y. S.; Chen, Y. X.; Hu, N. H. *Organometallics* **2005**, *24*, 2502–2510.
(36) Mizuoka, K.; Ikeda, Y. *Radiochim. Acta* **2004**, *92*, 631–635.

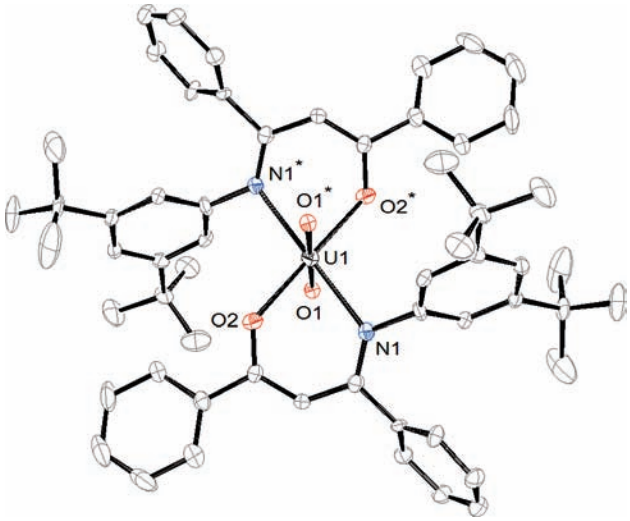

Figure 1. Oak Ridge Thermal Ellipsoid Plot (ORTEP) diagram of $UO_2(^{Ar}acnac)_2$ (Ar = 3,5-$^tBu_2C_6H_3$) (**2**·$2C_7H_8$) with 50% probability ellipsoids. Selected bond lengths (Å) and angles (deg): U1−O1 = 1.755(5), U1−O2 = 2.255(5), U1−N1 = 2.449(6), O1−U1−O1* = 180, O2−U1−N1 = 73.4(2), O2−U1−N1* = 106.6(2), O1−U1−O2 = 89.7(2), O1−U1−N1 = 86.6(2).

groups of the ^{t}Bu moieties, while the proton attached to the γ-carbon of the ketoiminate ring is observed at 6.21 ppm. The IR spectra of complexes **1** and **2** (as KBr mulls) exhibit ν_{asym}(U=O) vibrations at 908 cm^{-1} and 911 cm^{-1}, respectively. These values are typical of uranyl(VI).[38,39]

Complex **2** crystallizes in the triclinic space group $P\bar{1}$ as a toluene solvate, **2**·$2C_7H_8$, and its solid-state molecular structure is shown in Figure 1. Complex **2** exhibits an octahedral geometry with the two β-ketoiminate ligands occupying the uranyl equatorial plane (O1−U1−O2 = 89.7(2)°, O1−U1−N1 = 86.6(2)°). Moreover, the two *N*-aryl substituents exhibit a *trans* orientation. The U−O(oxo) bond length (U1−O1 =1.775(5) Å) is typical of the uranyl fragment, while the U−O(acnac) and U−N bond lengths are U1−O2 = 2.255(5) Å and U1−N1 = 2.449(6) Å, respectively. The aryl substituents of the β-ketoiminate ligand lie orthogonal to the uranyl equatorial plane, as is typically observed with β-diketiminate complexes.[40] The aryl substituents are also tilted toward the uranyl moiety as indicated by the relatively short U−C_{ipso} contact (3.233(7) Å), providing excellent steric protection of the equatorial plane. The N_2O_2 equatorial ligand environment provides a close match to that observed in the previously isolated complex UO_2(Ar$_2$nacnac)(acac).[18] Not surprisingly, the U−N and U−O bond lengths in **2** also mirror those observed in UO_2(Ar$_2$nacnac)(acac).

The bright orange color of **1** and **2** can be attributed to the prominent shoulders at 455 nm (ε = 2330 L·mol^{-1}·cm^{-1}) and 493 nm (ε = 1040 L·mol^{-1}·cm^{-1}), in their respective UV/vis spectra. These features may be due to the

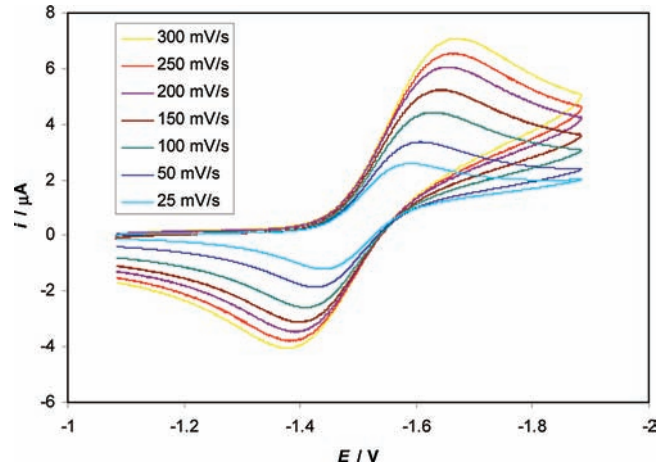

Figure 2. Room temperature cyclic voltammogram for **1** in CH_2Cl_2 (vs Fc/Fc^+, 0.1 M $[NBu_4][PF_6]$ as supporting electrolyte).

uranyl chromophore.[41] Complex **1** also exhibits a strong absorption at 355 nm (ε = 31200 L·mol^{-1}·cm^{-1}). This absorption is red-shifted in complex **2** to 383 nm (ε = 26000 L·mol^{-1}·cm^{-1}). Both are probably attributable to a ligand-to-metal charge transfer (LMCT) transition. The uncomplexed ligand, H(^{Ar}acnac) (Ar = 3,5-^{t}BuC_6H_3), also exhibits a strong absorption in this region (386 nm, ε = 13800 L·mol^{-1}·cm^{-1}), but the molar absorptivity is considerably lower.

The solution redox properties of complexes **1** and **2** have been investigated by cyclic voltammmetry. The cyclic voltammogram of **1** in CH_2Cl_2 reveals a reversible reduction feature at $E_{1/2}$ = −1.52 V (vs Fc/Fc^+) which we attribute to the UO_2^{2+}/UO_2^+ redox couple (Figure 2). This potential is similar to that observed for UO_2(Ar$_2$nacnac)(dbm) (dbm = PhC(O)CHC(O)Ph).[18] For complex **2**, the cyclic voltammogram in CH_2Cl_2 reveals a quasi-reversible reduction feature at −1.35 V (vs Fc/Fc^+). Notably, the difference in potential between the cathodic and anodic waves is large (0.29 V at 100 mV/s), and increases with increasing scan rate. Similar electrochemical behavior has been seen for other uranyl complexes.[42] When $[NBu_4][B\{C_6F_5\}_4]$ is used as the supporting electrolyte we observe a second reduction feature in the cyclic voltammogram of **2** (see Supporting Information). At a scan rates of 50 mV/s this feature is irreversible and is centered at −2.06 V (vs Fc/Fc^+). When the scan rate is increased to 200 mV/s an anodic wave appears in the cyclic voltammogram ($i_{p,c}/i_{p,a}$ = 1.64), suggesting that this feature approaches electrochemical reversibility as the scan rate increases.

In-line with the cyclic voltammetry results, **1** and **2** react with Cp^*_2Co to generate tractable uranyl(V) complexes, namely $[Cp^*_2Co][UO_2(^{Ar}acnac)_2]$ (Ar = 2,4,6-$Me_3C_6H_2$, **3**; 3,5-^{t}Bu$_2C_6H_3$, **4**), in moderate to good yields (eq 3). Both complexes contain the paramagnetic uranyl(V) moiety, as indicated by NMR spectroscopy. For instance, the ^{1}H NMR spectrum of **3** exhibits a broad resonance at −0.29 ppm, which we attribute to the para methyl substituent of the mesityl ring, while a broad resonance at 2.82 ppm is

(37) Mizuoka, K.; Tsushima, S.; Hasegawa, M.; Hoshi, T.; Ikeda, Y. *Inorg. Chem.* **2005**, *44*, 6211–6218.
(38) Berthet, J.-C.; Nierlich, M.; Ephritikhine, M. *Dalton Trans.* **2004**, 2814–2821.
(39) Berthet, J.-C.; Nierlich, M.; Ephritikhine, M. *Chem. Commun.* **2004**, 870–871.
(40) Bourget-Merle, L.; Lappert, M. F.; Severn, J. R. *Chem. Rev.* **2002**, *102*, 3031–3065.
(41) Baird, C. P.; Kemp, T. J. *Prog. React. Kinet.* **1997**, *22*, 87–139.
(42) Morris, D. E. *Inorg. Chem.* **2002**, *41*, 3542–3547.

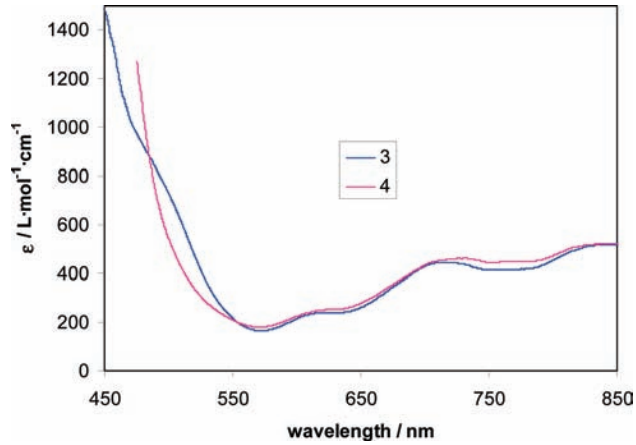

Figure 3. UV/vis spectra of **3** (1.6×10^{-3} M, blue line), and **4** (1.7×10^{-3} M, pink line) in CH_2Cl_2.

assignable to the ortho methyl substituents. Similarly, the ^{1}H NMR spectrum of **4** exhibits a broad resonance at −0.06 ppm, which we attribute to the *tert*-butyl substituents of the aryl group.

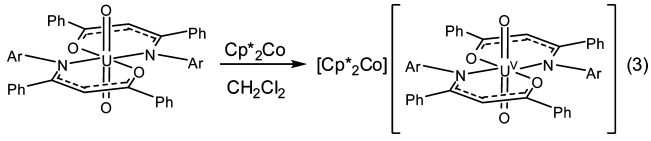

Ar = 2,4,6-$Me_3C_6H_2$, **3**; 3,5-$^t Bu_2C_6H_3$, **4**

The UV/vis spectra of complexes **3** and **4** in CH_2Cl_2 can be found in Figure 3. The spectra exhibit absorptions that are consistent with f→f transitions and the presence of a $5f^1$ ion. For instance, complex **3** exhibits transitions in the visible region, at 618 nm (ε = 250 L·mol^{-1}·cm^{-1}), 718 nm (ε = 460 L·mol^{-1}·cm^{-1}), and 843 nm (ε = 520 L·mol^{-1}·cm^{-1}). A nearly identical spectrum is observed for complex **4**. Both spectra mirror those observed for [Cp*$_2$Co][U(Ar$_2$nacnac)(acac)],[18] and other uranyl(V) complexes.[19,37] The IR spectra of complex **3**, recorded as a KBr pellet, is also consistent with the presence of the uranyl(V) ion. For **3**, the asymmetric stretch of the uranyl group is assigned to the peak at 784 cm^{-1} (which is 124 cm^{-1} lower than the asymmetric stretch observed for **1**). However, no peak in the IR spectrum of **4** could be definitively identified as the ν_{asym}(U═O) stretch, possibly because of overlap with the ligand vibrations.[5] We have also measured the magnetic susceptibility of complexes **3** and **4** in CD_2Cl_2 by Evans method.[43,44] Complex **3** displays an effective magnetic moment of 1.5 μ_B at room temperature, which is less than the theoretical value calculated for a $5f^1$ ion using the L-S coupling scheme (μ_{eff} = 2.57 μ_B).[45] Complex **4** displays a similar effective magnetic moment (μ_{eff} = 1.6 μ_B). Both values are within the range of effective magnetic moments previously measured for the UO_2^+ion.[22]

Complex **4** was found to crystallize in the monoclinic space group $P2_1/c$ as a dichloromethane and hexane solvate, **4**·2C_6H_{14}·4CH_2Cl_2. Its solid-state molecular structure is shown in Figure 4. Complex **4** consists of discrete cation/anion pairs: the closest intermolecular contact between the uranyl complex and the decamethylcobaltocene cation is C37−O1 = 3.41 Å. Like **2**, complex **4** possesses a distorted octahedral geometry. The U−O(oxo) bond length is 1.838(5) Å and the O1−U1−O1* angle is 180°. This distance is longer than that observed in complex **2** but on par with those observed in other uranyl(V) complexes.[1,9,19] In addition, the U−O(acnac) and U−N bond lengths are 2.364(6) Å and 2.513(6) Å, respectively. Both of these distances are also longer than those observed in **2**, which is consistent with the presence of the larger U^{5+} ion. Complex **4** also exhibits a short U−C_{ipso} contact (3.21 Å).

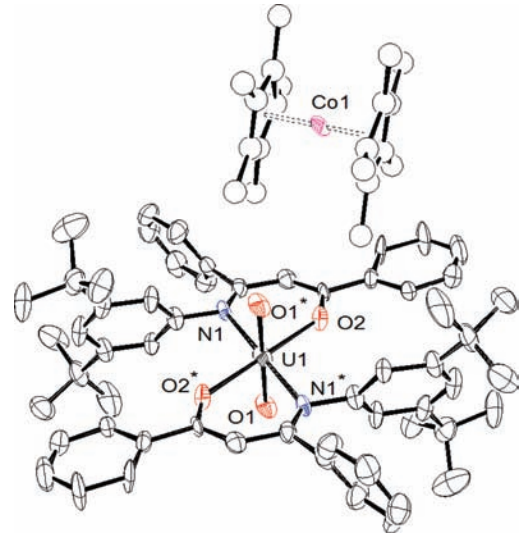

Figure 4. ORTEP diagram of [Cp*$_2$Co][UO_2(^{Ar}acnac)$_2$] (**4**·2C_6H_{14}·4CH_2Cl_2) with 50% probability ellipsoids. Selected bond lengths (Å) and angles (deg): U1−O1 = 1.838(5), U1−O2 = 2.364(6), U1−N1 = 2.513(6), O1−U1−O1* = 180, O2−U1−N1* = 109.6(2), O2−U1−N1 = 70.4(2), O1−U1−O2 = 88.7(2), O1−U1−N1 = 88.4(2).

Not surprisingly, complexes **3** and **4** are very air- and moisture-sensitive. In addition, they are thermally unstable. For instance, solutions of **4** in CD_2Cl_2 almost completely decompose after standing for 24 h at room temperature. Similar behavior is observed for the uranyl(V) Ar$_2$nacnac complexes, suggesting that changing the β substituents (from Me to Ph) in the ligand backbone has no effect on the overall stability of these species.[18] Given the cyclic voltammogram of complex **2** we have also explored the reduction of **4**. Thus reaction of **4** with Cp*$_2$Co in CH_2Cl_2 results in a slow color change to red; however, the only tractable product that can be isolated from these reaction mixtures is the uncomplexed ligand, H(^{Ar}acnac).

We have also studied the reactivity of our uranyl(VI) β-ketoiminate complexes, **1** and **2**, with B(C_6F_5)$_3$. Addition of 2 equiv of B(C_6F_5)$_3$ to **1**in CD_2Cl_2 results in no obvious interaction between the two molecules, as determined by ^{1}H and ^{19}F{^{1}H} NMR spectroscopies. However, reaction of **2** (which contains *tert*-butyl substituents at the relatively remote 3 and 5 positions of the aryl ring) with 2 equiv of B(C_6F_5)$_3$ in CH_2Cl_2 results is a rapid color change from orange to brown (Scheme 1). Layering this solution with hexanes and cooling to −25 °C leads to the isolation of UO(OB{C_6F_5}$_3$)(^{Ar}acnac)$_2$ (**5**) as a brown crystalline solid in good

(43) Evans, D. F. *J. Chem. Soc.* **1959**, 2003–2005.
(44) Cai, S.; Walker, F. A.; Licoccia, S. *Inorg. Chem.* **2000**, *39*, 3466–3478.
(45) Cotton, S. *Lanthanide and Actinide Chemistry*; John Wiley & Sons Ltd.: West Sussex, England, 2006.

Scheme 1

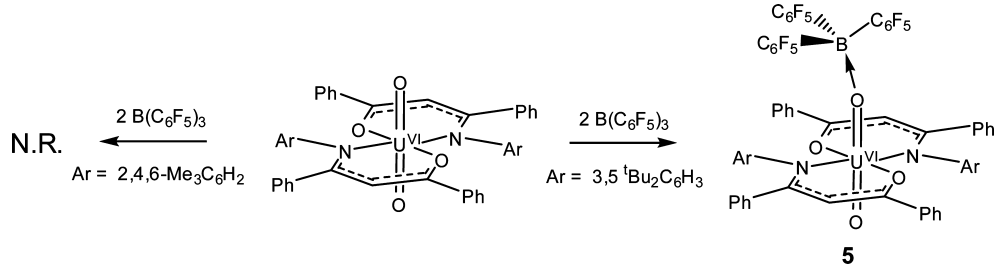

yield. When only 1 equiv of $B(C_6F_5)_3$ is used in the reaction with **2**, complex **5** is still formed; however, the isolated yields are markedly lower.

The ^{1}H NMR spectrum of **5** is qualitatively similar to that observed for **2**, but it exhibits modest changes to the chemical shifts. One notable feature of its ^{1}H NMR spectrum is a broadening of the signal associated with the ortho protons of the 3,5-^{t}Bu$_2$-C_6H_3 aryl substituent, possibly because of a decreased rate of rotation caused by coordination of $B(C_6F_5)_3$. The ^{19}F{^{1}H} NMR spectrum of **5** in C_6D_6 consists of 3 peaks in 2:1:2 ratio at −68.3, −94.0, −100.8, respectively, consistent with the incorporation of $B(C_6F_5)_3$ into the product. In addition, the resonance at −94.0 ppm (attributable to *p*-F) is considerably broadened relatively to that observed for the *p*-F resonance in uncoordinated $B(C_6F_5)_3$. For comparison, the ^{19}F{^{1}H} NMR spectrum of $B(C_6F_5)_3$ (in CD_2Cl_2) consists of 3 peaks in 2:1:2 ratio at −64.2, −80.0, −96.8, respectively; quite different from those observed for **5**. No signal was observed in the ^{11}B{^{1}H} NMR spectrum of **5**. The IR spectrum of **3** exhibits a medium intensity peak at 845 cm^{-1} which we have assigned to the ν_{asym}(U=O) vibration. This is in-line with the IR spectrum observed for the other known uranyl $B(C_6F_5)_3$ adduct.[3] Complex **5** quickly reacts with equimolar amounts of THF in C_6D_6, generating **2** and (THF)$B(C_6F_5)_3$, as determined ^{1}H NMR spectroscopy. This reaction is accompanied by a rapid color change from brown to orange as complex **2** is formed.

We have also measured the redox properties of **5** by cyclic voltammetry. Complex **5** was generated in situ in an electrochemical cell by addition of $B(C_6F_5)_3$ to complex **2**. Before the addition of $B(C_6F_5)_3$, we observe two redox couples (one at −1.35 V and one at about −2.0 V), as anticipated for complex **2**. After addition of 2 equiv of $B(C_6F_5)_3$, the features characteristic of complex **2** disappear and two new features appear: one at −0.78 V (vs Fc/Fc$^+$, 100 mV/s scan rate) and another at 1.79 V (vs Fc/Fc$^+$, 100 mV/s scan rate). Both features are irreversible up to scan rates of 2 V/s. We attribute the feature at −0.78 V to the one-electron reduction of complex **5**, while we attribute the feature at −1.79 V to the reduction of unreacted $B(C_6F_5)_3$.[46,47] Interestingly, the reduction potential for complex **5** is approximately 700 mV lower than that observed for **2**, consistent with the removal of electron density from the uranyl moiety by coordination of $B(C_6F_5)_3$.

Complex **5** crystallizes in the triclinic space group $P\bar{1}$ as a hexane solvate, **5**·C_6H_{14}. Its solid-state molecular structure is shown in Figure 5. The uranium center in **5** exhibits an octahedral coordination geometry, with one $B(C_6F_5)_3$ moiety coordinated to an oxo ligand of uranyl. The U−O bond length of the complexed oxo ligand is 1.890(4) Å, which is 0.135 Å longer than the U−O bond length observed in **2**. The other uranium oxo ligand exhibits a bond length of U1−O1= 1.777(4) Å, demonstrating the coordination of $B(C_6F_5)_3$ has little effect on the uncomplexed oxo ligand. In addition, the uranyl moiety in **5** remains linear (O1−U1−O2 = 177.2(2)°). The $B(C_6F_5)_3$ unit exhibits the anticipated tetrahedral coordination environment with a B1−O2 bond length of 1.584(7) Å. Finally, the U−N bond lengths in **5** are U1−N1 = 2.397(5) Å and U1−N2 = 2.417(5) Å, while the U−O(acnac) bond lengths are U1−O3 = 2.192(4) Å and U1−O4 = 2.194(4) Å.

The metrical parameters of **5** are similar to those observed in the previously reported $B(C_6F_5)_3$-uranyl adduct, UO{OB-$(C_6F_5)_3$}$(NCN)_2$ [NCN = $(Me_3SiN)CPh(NSiMe_3)$].[3] This complex exhibits U−O bond lengths of 1.898(3) Å and 1.770(3) Å for the $B(C_6F_5)_3$-complexed and uncomplexed oxo ligands, respectively, while the B−O bond length was found to be 1.545(6) Å. There are also several examples of $B(C_6F_5)_3$ coordinating to an oxo ligand of a transition-metal oxo complex.[48−51] In these molecules the M=O bond is

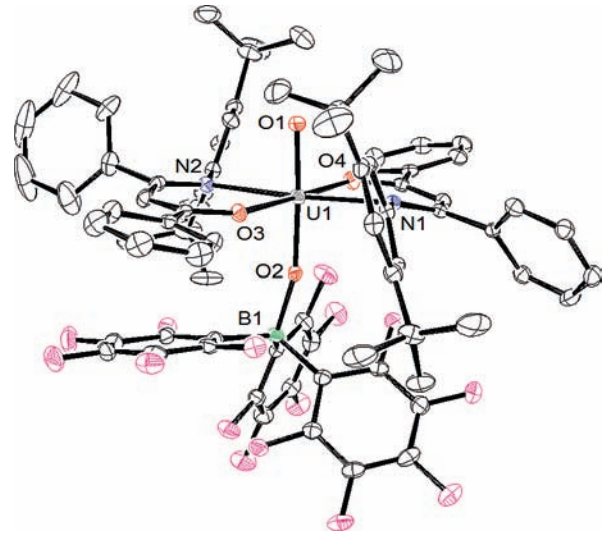

Figure 5. ORTEP diagram of UO(OB{C_6F_5}$_3$)(^{Ar}acnac)$_2$ (**5**·C_6H_{14}) with 30% probability ellipsoids. Selected bond lengths (Å) and angles (deg): U1−O1 = 1.777(4), U1−O2 = 1.890(4), U1−N1 = 2.397(5), U1−N2 = 2.417(5), U1−O3 = 2.192(4), U1−O4 = 2.194(4), B1−O2 = 1.584(7), O1−U1−O2 = 177.2(2), O3−U1−N1 = 109.8(2), O4−U1−N2 = 106.0(2), N2−U1−O3 = 73.0(2), N1−U1−O4 = 71.2(2), O1−U1−O3 = 91.0(2), O1−U1−O4 = 88.4(2), O1−U1−N1 = 90.4(2), O1−U1−N2 = 86.3(2), B1−O2−U1 = 163.7(4).

typically elongated by approximately 0.1 Å upon coordination of $B(C_6F_5)_3$,[49−51] while the B−O bond length is approximately 1.53 Å.[48−50]

The structural characterization of complexes **2**, **4**, and **5** permits a thorough comparison of the metrical parameters of the uranyl moiety after coordination of a Lewis acid or after reduction to U(V). In both modes of reactivity, we see that the two oxo ligands of the uranyl fragment do not deviate from their usual *trans* arrangement, while the acnac ligands are not displaced out of the equatorial plane. However in both **4** and **5**, the U−O(oxo) bond lengths diverge from their typical values. For instance, the U−O(oxo) bond length in **4** is about 0.08 Å longer that observed in **2**, while the U−O($B(C_6F_5)_3$) bond length in **5** is about 0.14 Å longer than the U−O bond length of the parent complex. Interestingly, we also observe a slight decrease in the U−O(acnac) distances upon coordination of $B(C_6F_5)_3$. In particular, the U−O(acnac) distances in **5** are about 0.05 Å shorter than that observed in **2**, which we attribute to the removal of electron density from the uranyl center by $B(C_6F_5)_3$.

Summary

The successful isolation of complexes **3** and **4** demonstrates that a β-ketoiminate ligand set is capable of supporting the reactive uranyl(V) moiety. However, even with our carefully tailored ligand set, both **3** and **4** are still thermally unstable, a characteristic they share with most of the uranyl(V) complexes isolated thus far. However, the stability of **3** and **4** is greatly improved relative to that of UO_2^+(aq), likely because of the bulky, substitutionally inert equatorial ligand environment. The protection of the uranyl equatorial plane by the aryl substituent of ^{Ar}acnac is readily demonstrated by the short U−C_{ipso} carbon distances observed in the solid-state molecular structures of **2**, **4**, and **5**. Moreover, the lack of reactivity between **1** and $B(C_6F_5)_3$ confirms that a bulky aryl substitutent (which projects bulk above and below the uranyl equatorial plane) can curtail the ability of a Lewis acid to interact with the uranyl oxygen atoms. This lack of reactivity is most likely a steric phenomenon as $B(C_6F_5)_3$ can interact with the uranyl oxo ligands in the less sterically encumbered analogue **2**. Finally, inspection of the solid-state molecular structures of **4** and **5**, suggest that their oxo ligands are more activated toward substitution than those of the parent complex. Future studies will focus on attempts to functionalize the oxo ligands in UO_2^+, particularly efforts to cleave the U−O bond in a well-defined manner.

Experimental Section

General Procedures. All reactions and subsequent manipulations were performed under anaerobic and anhydrous conditions under either a high vacuum or an atmosphere of nitrogen or argon. THF, hexanes, diethyl ether, and toluene were dried by passage over activated molecular sieves using a Vacuum Atmospheres solvent purification system. C_6D_6, CD_2Cl_2, and THF-d_8 were dried over activated 4 Å molecular sieves for 24 h before use. $B(C_6F_5)_3$ was made by the published procedure, except that pentafluoroiodoobenzene was used in place of pentafluorobromobenzene.[52] $UO_2Cl_2(THF)_3$[53] and $NBu_4[B\{C_6F_5\}_4]$[54] were synthesized by the published procedures. Cp^*_2Co was recrystallized from hexanes before use, while all other reagent were purchased from commercial suppliers and used as received.

NMR spectra were recorded on a Varian INOVA 400 or Varian INOVA 500 spectrometer. ^{1}H and $^{13}C\{^1H\}$ NMR spectra are referenced to external $SiMe_4$ using the residual protio solvent peaks as internal standards (^{1}H NMR experiments) or the characteristic resonances of the solvent nuclei (^{13}C NMR experiments). $^{19}F\{^1H\}$ NMR spectra were referenced to external α,α,α-trifluorotoluene. Elemental analyses were performed by the Microanalytical Laboratory at UC Berkeley. UV−vis spectra were recorded on an Ocean Optics USB4000 UV−vis spectrometer equipped with a USB-DT light source and IR spectra were recorded on a Mattson Genesis FTIR spectrometer.

Cyclic Voltammetry (CV) Measurements. CV experiments were performed with a CH Instruments 600c Potentiostat, and the data were processed using CHI software (version 6.29). All experiments were performed in a glovebox using a 20 mL glass vial as the cell. The working electrode consisted of a platinum disk embedded in glass (2 mm diameter), the counter electrode was a platinum wire, and the reference electrode consisted of AgCl plated on Ag wire. Solutions employed during CV studies were typically 3 mM in the uranium complex and 0.1 M in $[Bu_4N][PF_6]$. All potentials are reported versus the $[Cp_2Fe]^{0/+}$ couple. For all trials $i_{p,a}/i_{p,c} = 1$ for the $[Cp_2Fe]^{0/+}$ couple, while $i_{p,c}$ increased linearly with the square root of the scan rate (i.e., $\sqrt{\upsilon}$). Redox couples which exhibited behavior similar to the $[Cp_2Fe]^{0/+}$ couple were thus considered reversible.

{2,4,6-$Me_3C_6H_2$}NHC(Ph)=CHC(Ph)O. A round-bottom flask was charged with dibenzoylmethane (3.20 g, 14.3 mmol), mesitylaniline (1.98 g, 14.6 mmol), and $Zn(OTf)_2$ (50 mg). Toluene (25 mL) was added, and the resulting solution was refluxed for 72 h. The volatiles were removed by distillation to provide an orange oil, which was subsequently dissolved in hexanes (20 mL). This solution was washed successively with 1 M NaOH (20 mL) and 1 M HCl (20 mL) and then dried over $MgSO_4$. The volatiles were then removed in vacuo to provide a yellow oil. 1.06 g, 21% yield. ^{1}H NMR ($CDCl_3$, 25 °C, 500 MHz): δ 2.14 (s, 6H, Me), 2.19 (s, 3H, Me), 6.10 (s, 1H, γ-CH), 6.74 (s, 2H, meta CH), 7.18−7.27 (m, 5H, aryl CH), 7.44 (m, 3H, aryl CH), 7.98 (m, 2H, ortho CH), 12.68 (s, 1H, NH). $^{13}C\{^1H\}$ NMR ($CDCl_3$, 25 °C, 125 MHz): δ 18.7 (Me), 20.8 (Me), 93.8 (γ-C), 127.1, 127.7, 127.9, 128.2, 128.9, 129.5, 130.9, 134.3, 134.4, 136.1, 136.2, 140.1, 164.9 (β-CN), 189.0 (β-CO). ESI-MS: *m/z* 342 $(M+H)^+$.

(46) Kwaan, R. J.; Harlan, C. J.; Norton, J. R. *Organometallics* **2001**, *20*, 3818–3820.
(47) Harlan, C. J.; Hascall, T.; Fujita, E.; Norton, J. R. *J. Am. Chem. Soc.* **1999**, *121*, 7274–7275.
(48) Sánchez-Nieves, J.; Royo, P.; Mosquera, M. E. G. *Eur. J. Inorg. Chem.* **2006**, *2006*, 127–132.
(49) Galsworthy, J. R.; Green, M. L. H.; Müller, M.; Prout, K. *Dalton Trans.* **1997**, 1309–1314.
(50) Doerrer, L. H.; Galsworthy, J. R.; Green, M. L. H.; Leech, M. A. *Dalton Trans.* **1998**, 2483–2488.
(51) Doerrer, L. H.; Galsworthy, J. R.; Green, M. L. H.; Leech, M. A.; Müller, M. *Dalton Trans.* **1998**, 3191–3194.
(52) Chernega, A. N.; Graham, A. J.; Green, M. L. H.; Haggit, J.; Lloyd, J.; Mehnert, C. P.; Metzler, N.; Souter, J. *Dalton Trans.* **1997**, 2293–2303.
(53) Wilkerson, M. P.; Burns, C. J.; Paine, R. T.; Scott, B. L. *Inorg. Chem.* **1999**, *38*, 4156–4158.
(54) LeSuer, R. J.; Buttolph, C.; Geiger, W. E. *Anal. Chem.* **2004**, *76*, 6395–6401.

{3,5-^{t}Bu$_2$C$_6$H$_3$}NHC(Ph)=CHC(Ph)O. To a vial charged with a stir bar was added dibenzoylmethane (0.1792 g, 0.80 mmol), 3,5-di-*tert*-butylaniline (0.1652 g, 0.80 mmol), and $Zn(OTf)_2$ (10 mg). The mixture of the two solids was warmed to 70 °C on a hot plate resulting in the formation of an orange oil. After stirring for 18 h the orange oil had solidified. Water (2 mL), and CH_2Cl_2 (2 mL) were added to the solid to give an orange organic solution below a colorless aqueous layer. The organic layer was then isolated and dried with $MgSO_4$, and all volatiles were removed in vacuo to provide an orange oil, 0.306 g, 93% yield. ^{1}H NMR ($CDCl_3$, 25 °C, 500 MHz): δ 1.06 (s, 18H, Me), 5.99 (s, 1H, γ-CH), 6.55 (d, 2H, J_{HH} = 1.5 Hz, ortho CH), 6.96 (s, 1H, para CH), 7.21−7.39 (m, 6H, meta and para CH), 7.90 (m, 4H, ortho CH), 12.98 (s, 1H, NH). ^{13}C{^{1}H} NMR ($CDCl_3$, 25 °C, 125 MHz): δ 31.1 (Me), 34.5 (*C*Me$_3$), 96.3 (γ-C), 109.9, 117.4, 127.0, 128.1, 128.2, 128.4, 129.3, 131.0, 136.1, 138.2, 139.9, 151.0, 151.7 (β-CN), 161.6 (β-CO). ESI-MS: *m*/*z* 412 (M+H)$^+$. UV/vis (CH_2Cl_2, 7.8 × 10^{-5} M): 386 nm (ε = 13800 L·mol^{-1}·cm^{-1}).

UO$_2$(^{Ar}acnac)$_2$ (Ar = 2,4,6-Me$_3$C$_6$H$_2$) (1). To a stirring toluene suspension (3 mL) containing $UO_2Cl_2(THF)_3$ (0.1803 g, 0.32 mmol) was added Li[{2,4,6-Me$_3$C$_6$H$_2$}*N*C(Ph)=CHC(Ph)*O*] (0.225 g, 0.64 mmol), which was prepared by deprotonation of {2,4,6-Me$_3$C$_6$H$_2$}-NHC(Ph)=CHC(Ph)O with 1 equiv of *n*-BuLi. This resulted in the immediate formation of an orange solution concomitant with the formation of an orange powder. After stirring for 1 h, the volatiles were removed in vacuo and the resulting oil was dissolved in CH_2Cl_2 (10 mL). This mixture was filtered through a Celite column supported on glass wool (0.5 cm × 2 cm). The volume of the filtrate was reduced in vacuo, and the solution was layered with an equal volume of hexanes. Storage of this solution at −25 °C for 1 week resulted in the deposition of an orange powder, which was collected by decanting off the supernatant (0.1496 g). Further concentration of the supernatant resulted in the deposition of a further 0.0295 g of orange powder, for a total of 0.1791 g, 58% yield. Anal. Calcd for $C_{48}H_{44}N_2O_4U$: C, 60.63; H, 4.66; N, 2.95. Found: C, 59.13; H, 4.42; N, 3.41. ^{1}H NMR (C_6D_6, 25 °C, 400 MHz): δ 2.20 (s, 6H, Me), 2.23 (s, 12H, Me), 6.08 (s, 2H, γ-CH), 6.77 (s, 4H, meta CH), 7.00 (m, 6H, aryl CH), 7.26 (m, 6H, aryl CH), 7.34 (m, 4H, aryl CH), 7.75 (d, 4H, J_{HH} = 7.2 Hz, ortho CH). ^{1}H NMR (CD_2Cl_2, 25 °C, 400 MHz): δ 2.23 (s, 12H, Me), 2.42 (s, 6H, Me), 6.15 (s, 2H, γ-CH), 6.97 (s, 4H, meta CH), 7.29−7.35 (m, 6H, aryl CH), 7.45−7.52 (m, 10H, aryl CH), 7.85 (d, 4H, J_{HH} = 7.2 Hz, ortho CH). ^{13}C{^{1}H} NMR (CD_2Cl_2, 25 °C, 125 MHz): δ 19.1 (Me), 21.3 (Me), 100.9 (γ-C), 127.9, 128.0, 128.5, 128.8, 130.2, 131.1, 134.7, 137.2, 138.6, 139.5, 173.5 (β-CN), 178.1 (β-CO). UV/vis (CH_2Cl_2, 1.2 × 10^{-5} M): 288 nm (sh, ε = 19300 L·mol^{-1}·cm^{-1}), 355 nm (ε = 31200 L·mol^{-1}·cm^{-1}), 455 nm (sh, ε = 2330 L·mol^{-1}·cm^{-1}). IR (KBr pellet, cm^{-1}): 1587(m), 1557(s), 1495(s), 1469(s), 1439(s), 1380(s), 1297(m), 1278(m), 1213(m), 1185(w), 1159(w), 1116(w), 1063(m), 1024(m), 908(s) ν_{asym} (U=O), 857(m), 832(w), 811(w), 777(m), 767(m), 720(m), 693(m), 627(m), 574(m), 533(m).

UO$_2$(^{Ar}acnac)$_2$ (Ar = 3,5-^{t}Bu$_2$C$_6$H$_3$) (2). To a stirring Et_2O solution (3 mL) of {3,5-^{t}Bu$_2$C$_6$H$_3$}NHC(Ph)=CHC(Ph)O (0.306 g, 0.74 mmol) was added NaN{SiMe$_3$}$_2$ (0.138 g, 0.75 mmol). After 10 min of stirring, $UO_2Cl_2(THF)_3$ (0.207 g, 0.37 mmol) was added, and the solution was stirred for a further 2 h, resulting in the deposition of an orange powder. The solution was decanted off, and the powder was dissolved in toluene (5 mL). This mixture was filtered through a Celite column supported on glass wool (0.5 cm × 2 cm). The solution was then layered with an equal volume of hexanes, and the volume of the solution was reduced in vacuo resulting in the deposition of an orange microcrystalline powder. The powder was collected by decanting off the supernatant, providing 0.1062 g. A further 0.041 g of powder was collected by concentrating the original reaction mixture and cooling to −25 °C for 24 h. Total yield: 0.1472 g, 36% yield. Anal. Calcd for $C_{58}H_{64}N_2O_4U\cdot C_7H_8$: C, 65.98; H, 6.13; N, 2.37. Found: C, 66.59; H, 5.97; N, 2.22. ^{1}H NMR (CD_2Cl_2, 25 °C, 500 MHz): δ 1.11 (s, 36H, Me), 6.21 (s, 2H, γ-H), 7.03 (s, 4H, ortho aryl CH), 7.27−7.34 (m, 12H, aryl CH), 7.43 (m, 6H, aryl CH), 7.53 (d, J_{HH} = 7.0 Hz, 4H, ortho CH). ^{13}C{^{1}H} NMR (CD_2Cl_2, 25 °C, 125 MHz): δ 31.4 (Me), 35.4 (*C*Me$_3$), 100.7 (γ-C), 121.0, 122.6, 128.0, 128.6, 128.7, 128.8, 129.5, 130.9, 139.5, 141.5, 142.1, 152.9, 173.1 (β-CN), 178.8 (β-CO). UV/vis (CH_2Cl_2, 2.8 × 10^{-5} M): 285 nm (sh, ε = 17100 L·mol^{-1}·cm^{-1}), 383 nm (ε = 26000 L·mol^{-1}·cm^{-1}), 493 nm (sh, ε = 1040 L·mol^{-1}·cm^{-1}). IR (KBr pellet, cm^{-1}): 1590(s), 1556(s), 1497(s), 1483(s), 1450(m), 1383(s), 1371(m), 1298(m), 1247(w), 1073(w), 1025(w), 932(w), 911(m) ν_{asym}(U=O), 905(w), 873(w), 759(w), 737(w), 715(w), 697(m), 609(w), 577(w).

[Cp*$_2$Co][UO$_2$(^{Ar}acnac)$_2$] (Ar = 2,4,6-Me$_3$C$_6$H$_2$) (3). To a stirring solution of **1** (0.0582 g, 0.061 mmol) in CH_2Cl_2 was added Cp*$_2$Co (0.0207 g, 0.063 mmol). The solution immediately turned green-brown. After 10 min of stirring the solution was filtered through a Celite column supported on glass wool (0.5 cm × 2 cm). The supernatant was then layered with an equal volume of hexanes. Storage of this solution at −25 °C for 48 h resulted in the deposition of a yellow-brown powder, which was collected by decanting off the supernatant (0.0462 g, 59% yield). Anal. Calcd for $C_{68}H_{74}CoN_2O_4U$: C, 63.79; H, 5.83; N, 2.19. Found: C, 63.38; H, 5.74; N, 2.52. ^{1}H NMR (CD_2Cl_2, 25 °C, 400 MHz): δ −0.29 (br s, 6H, Me), 2.22 (s, 30H, C_5Me_5), 2.82 (br s, 12H, Me), 3.33 (br s, 4H, aryl CH), 3.59 (br s, 2H, γ-CH), 4.41 (br s, 4H, aryl CH), 5.27 (br s, 4H, aryl CH), 5.59 (br s, 4H, aryl CH), 6.32 (br s, 2H, aryl CH), 6.68 (br s, 2H, aryl CH), one set or aryl resonances was not observed. UV/vis (CH_2Cl_2, 1.6 × 10^{-3} M): 501 nm (sh, ε = 710 L·mol^{-1}·cm^{-1}), 618 nm (ε = 250 L·mol^{-1}·cm^{-1}), 718 nm (ε = 460 L·mol^{-1}·cm^{-1}), 843 nm (ε = 520 L·mol^{-1}·cm^{-1}). IR (KBr pellet, cm^{-1}): 1586(m), 1558(m), 1497(s), 1474(s), 1415(s), 1384(m), 1328(w), 1309(w), 1298(w), 1272(w), 1213(m), 1121(w), 1077(w), 1060(w), 1025(m), 908(w), 899(w), 858(w), 834(w), 784(s) ν_{asym}(U=O), 746(m), 695(m), 629(w).

[Cp*$_2$Co][UO$_2$(^{Ar}acnac)$_2$] (Ar = 3,5-^{t}Bu$_2$C$_6$H$_3$) (4). To a stirring solution of **2** (0.0384 g, 0.027 mmol) in CH_2Cl_2 was added Cp*$_2$Co (0.0125 g, 0.037 mmol). The solution immediately turned bright green. The solution was filtered through a Celite column supported on glass wool (0.5 cm × 2 cm), and the supernatant was then layered with an equal volume of hexanes. Storage of this solution at −25 °C for 24 h resulted in the deposition of a large green blocks, which were collected by decanting off the supernatant (0.0361 g, 72% yield). Anal. Calcd for $C_{78}H_{94}CoN_2O_4U$: C, 65.95; H, 6.67; N, 1.97. Found: C, 65.73; H, 6.58; N, 2.14. ^{1}H NMR (CD_2Cl_2, 25 °C, 400 MHz): δ −0.06 (br s, 36H, CMe$_3$), 0.09 (br s, 4H, aryl CH), 0.57 (br s, 2H, aryl CH), 1.64 (br s, 4H, aryl CH), 2.47 (s, 30H, C_5Me_5), 3.46 (br s, 2H, γ-CH), 4.20 (br s, 4H, aryl CH), 4.88 (br s, 4H, aryl CH), 5.41 (br s, 4H, aryl CH), 6.12 (br s, 2H, aryl CH), 6.42 (br s, 2H, aryl CH). UV/vis (CH_2Cl_2, 1.7 × 10^{-3} M): 620 nm (ε = 250 L·mol^{-1}·cm^{-1}), 725 nm (ε = 460 L·mol^{-1}·cm^{-1}), 846 nm (ε = 520 L·mol^{-1}·cm^{-1}). IR (KBr pellet, cm^{-1}): 1588(s), 1567(m), 1498(s), 1482(s), 1455(s) 1392(m), 1327(m), 1295(m), 1249(m), 1214(w), 1182(w), 1134(w), 1072(m), 1056(m), 1025(m), 988(w), 889(br m), 837(w), 758(sh), 714(m), 697(m), 617(w), 574(w).

UO(OB{C$_6$F$_5$}$_3$)(^{Ar}acnac)$_2$ (Ar = 3,5-^{t}Bu$_2$C$_6$H$_3$) (5). To a stirring solution of **2** (0.0517 g, 0.047 mmol) in CH_2Cl_2 (2 mL) was added $B(C_6F_5)_3$ (0.0477 g, 0.093 mmol). The solution immediately turned brown. Hexanes (4 mL) was added, and the

Table 1. X-ray Crystallographic Data for Complexes $2\cdot 2C_7H_8$, $4\cdot 2C_6H_{14}\cdot 4CH_2Cl_2$, and $5\cdot C_6H_{14}$

	$2\cdot 2C_7H_8$	$4\cdot 2C_6H_{14}\cdot 4CH_2Cl_2$	$5\cdot C_6H_{14}$
empirical formula	$C_{72}H_{80}N_2O_4U$	$C_{94}H_{130}CoCl_8N_2O_4U$	$C_{82}H_{78}BF_{15}N_2O_4U$
crystal habit, color	block, orange	block, green	cube, brown
crystal size (mm)	0.15 × 0.10 × 0.06	0.20 × 0.15 × 0.08	0.25 × 0.20 × 0.15
crystal system	triclinic	monoclinic	triclinic
space group	$P\bar{1}$	$P2_1/c$	$P\bar{1}$
volume (Å^3)	1540.6(5)	4778(2)	3783.6(7)
a (Å)	10.234(2)	13.376(1)	12.327(1)
b (Å)	11.042(2)	15.880(2)	13.855(2)
c (Å)	15.124(3)	22.599(2)	22.295(2)
α (deg)	70.187(3)	90	86.873(2)
β (deg)	88.089(3)	92.861(3)	85.589(2)
γ (deg)	73.812(3)	90	86.192(2)
Z	1	2	2
formula weight (g/mol)	1275.4	1932.6	1689.3
density (calculated) (Mg/m^3)	1.375	1.339	1.483
absorption coeff. (mm^{-1})	2.684	2.130	2.233
F_{000}	650	1990	1696
total no. reflections	12036	39651	33066
unique reflections	5795	9947	15422
final R indices [$I > 2\sigma(I)$]	$R_1 = 0.059$, $wR_2 = 0.139$	$R_1 = 0.080$, $wR_2 = 0.225$	$R_1 = 0.061$, $wR_2 = 0.145$
largest diff. peak and hole (e$^-$ Å^{-3})	1.42 and −1.71	3.27 and −3.07	4.01 and −2.11
GOF	0.968	1.080	1.016

volume of the solution was reduced in vacuo until incipient precipitation was observed. The solution was then layered with another aliquot of hexanes (2 mL). Storage of this solution at −25 °C for 24 h resulted in the deposition of a brown microcrystalline powder, which was collected by decanting off the supernatant (0.0617 g, 81% yield). Anal. Calcd for $C_{76}H_{64}BF_{15}N_2O_4U$: C, 56.94; H, 4.02; N, 1.75. Found: C, 55.49; H, 4.08; N, 1.85. ^{1}H NMR (C_6D_6, 25 °C, 500 MHz): δ 1.07 (s, 36H, Me), 5.92 (s, 2H, γ-H), 6.81 (t, $J_{HH} = 7.5$ Hz, 2H, para CH), 6.89 (t, $J_{HH} = 7.5$ Hz, 4H, meta CH), 7.03 (br s, 4H, ortho aryl CH), 7.17−7.22 (m, 12H, aryl CH), 7.34 (d, $J_{HH} = 7.5$ Hz, 4H, ortho CH). ^{19}F{^{1}H} NMR (C_6D_6, 25 °C, 276 MHz): δ −68.3 (br s, 6F, ortho CF), −94.0 (br s, 3F, para CF), −100.8 (br s, 6F, meta CF). ^{13}C{^{1}H} NMR (C_6D_6, 25 °C, 125 MHz): δ 31.3 (Me), 35.4 (*C*Me$_3$), 104.5 (γ-C), 123.0, 123.5, 128.0, 128.6, 129.3, 129.4, 132.0, 136.8 (br s, CF), 138.1, 138.8 (br s, CF), 140.5, 142.9, 147.4 (br s, CF), 149.3 (br s, CF), 153.1, 174.0 (β-CN), 178.1 (β-CO). IR (KBr pellet, cm^{-1}): 1647(m), 1597(m), 1558 (s), 1518(s), 1471(vs), 1365(s), 1298(s), 1247(m), 1211(w), 1192(w), 1095(s), 1025(m), 980(s), 921(m), 895(m), 845(m) ν_{asym}(U=O), 811(w), 705(s), 601(m), 577(m).

X-ray Crystallography. The solid-state molecular structures of complexes $2\cdot 2C_7H_8$, $4\cdot 2C_6H_{14}\cdot 4CH_2Cl_2$, and $5\cdot C_6H_{14}$ were determined similarly with exceptions noted in the following paragraph. Crystals were mounted on a glass fiber under Paratone-N oil. Data collection was carried out a Bruker 3-axis platform diffractometer with SMART-1000 CCD detector. The instrument was equipped with graphite monochromatized Mo Kα X-ray source ($\lambda = 0.71073$ Å). All data were collected at 150(2) K using Oxford nitrogen gas cryostream system. A hemisphere of data was collected using ω scans, with 15 s frame exposures and 0.3° frame widths. SMART[55] was used to determine the cell parameters and data collection. The raw frame data were processed using SAINT.[56] The empirical absorption correction was applied based on Psi-scan for $2\cdot 2C_7H_8$ and $5\cdot C_6H_{14}$ or SADABS for $4\cdot 2C_6H_{14}\cdot 4CH_2Cl_2$. Subsequent calculations were carried out using SHELXTL.[57] The structures were solved using Direct methods and difference Fourier techniques. All hydrogen atom positions were idealized and rode on the atom of attachment. The final refinement included anisotropic temperature factors on all non-hydrogen atoms. Structure solution, refinement, graphics, and creation of publication materials were performed using SHELXTL or WinGX.[58]

For complex $4\cdot 2C_6H_{14}\cdot 4CH_2Cl_2$, because of severe disorder in the molecules of solvation (identified as CH_2Cl_2 and hexane), the SQUEEZE function in PLATON was applied. However, one dichloromethane could be adequately modeled. For this molecule, the C−Cl bond lengths were fixed to 1.70(1) Å, and the Cl−Cl distance was fixed to 3.00(1) Å. The carbons of cyclopentadienyl ring of the $[Cp_2{*}Co]^+$ moiety also displayed a significant amount of thermal motion. For complex $5\cdot C_6H_{14}$, one *tert*-butyl group was found to be disordered between two positions about the tertiary carbon, in a 50:50 ratio. Restraints were applied to the disordered *tert*-butyl groups by fixing the C−C bond lengths between the tertiary and methyl carbons to 1.54(1) Å. In addition, a disordered molecule of hexanes was found in the crystal lattice. It was modeled in two different positions, in a 75:25 ratio. However, because of disorder, some of the carbon atoms could not be located. For this structure, the atoms of the solvent molecule were refined isotropically, while the hydrogen atoms were not assigned. A summary of relevant crystallographic data for $2\cdot 2C_7H_8$, $4\cdot 2C_6H_{14}\cdot 4CH_2Cl_2$, and $5\cdot C_6H_{14}$ is presented in Table 1.

Acknowledgment. We thank the University of California, Santa Barbara and the University of California Energy Institute for financial support of this work.

Supporting Information Available: X-ray crystallographic details (as CIF files) of $2\cdot 2C_7H_8$, $4\cdot 2C_6H_{14}\cdot 4CH_2Cl_2$, and $5\cdot C_6H_{14}$; tabulated cyclic voltammetry data for **1**, **2**, and **5**; UV/vis spectra for **1** and **2**; ^{1}H NMR spectra for complexes **1**−**5**. This material is available free of charge via the Internet at http://pubs.acs.org.

IC802360Y

(55) *SMART Software Users Guide*, Version 5.1; Bruker Analytical X-ray Systems, Inc.: Madison, WI, 1999.

(56) *SAINT Software Users Guide*, Version 5.1, Bruker Analytical X-ray Systems, Inc.: Madison, WI, 1999.

(57) Sheldrick, G. M. *SHELXTL*, Bruker Analytical X-ray Systems, Inc.: Madison, WI, 2001.

(58) Farrugia, L. J. *J. Appl. Crystallogr.* **1999**, *32*, 837–838.